Preclinical Profile of a Potent γ-Secretase Inhibitor Targeting Notch Signaling with *In vivo* Efficacy and Pharmacodynamic Properties

Leopoldo Luistro,[1] Wei He,[1] Melissa Smith,[1] Kathryn Packman,[1] Maria Vilenchik,[1] Daisy Carvajal,[1] John Roberts,[2] James Cai,[3] Windy Berkofsky-Fessler,[6] Holly Hilton,[6] Michael Linn,[4] Alexander Flohr,[7] Roland Jakob-Røtne,[7] Helmut Jacobsen,[8] Kelli Glenn,[5] David Heimbrook,[1] and John F. Boylan[1]

[1]Discovery Oncology, [2]Discovery Chemistry, [3]In Silico Sciences, [4]Non-clinical Safety, [5]Drug Metabolism, and [6]RNA Therapeutics, Hoffmann-La Roche, Inc., Nutley, New Jersey and [7]Discovery Chemistry and [8]CNS Research, Hoffmann-La Roche, Inc., Basel, Switzerland

Abstract

Notch signaling is an area of great interest in oncology. RO4929097 is a potent and selective inhibitor of γ-secretase, producing inhibitory activity of Notch signaling in tumor cells. The RO4929097 IC_{50} in cell-free and cellular assays is in the low nanomolar range with >100-fold selectivity with respect to 75 other proteins of various types (receptors, ion channels, and enzymes). RO4929097 inhibits Notch processing in tumor cells as measured by the reduction of intracellular Notch expression by Western blot. This leads to reduced expression of the Notch transcriptional target gene *Hes1*. RO4929097 does not block tumor cell proliferation or induce apoptosis but instead produces a less transformed, flattened, slower-growing phenotype. RO4929097 is active following oral dosing. Antitumor activity was shown in 7 of 8 xenografts tested on an intermittent or daily schedule in the absence of body weight loss or Notch-related toxicities. Importantly, efficacy is maintained after dosing is terminated. Angiogenesis reverse transcription-PCR array data show reduced expression of several key angiogenic genes. In addition, comparative microarray analysis suggests tumor cell differentiation as an additional mode of action. These preclinical results support evaluation of RO4929097 in clinical studies using an intermittent dosing schedule. A multicenter phase I dose escalation study in oncology is under way. [Cancer Res 2009;69(19):7672–80]

Introduction

Cancer is a disease characterized by uncontrolled proliferation stemming from aberrant regulation of cellular signaling. Cellular heterogeneity typical of tumors may be partly due to dysregulated differentiation (1). In recent years, developmental biology research has provided new insights in understanding the signals that control cancer. During development and tissue remodeling, a self-renewing pluripotent progenitor cell population serves as the source for all mature, differentiated cell types. A link between the characteristics of these pluripotent cells and the rapid uncontrolled proliferation of tumors is becoming clear (2). One major developmental signaling axis is the evolutionarily conserved Notch pathway (3–5). Notch signaling regulates cell fate decisions by mediating the homeostasis and differentiation of progenitor cells during development and self-renewal of adult pluripotent stem cells. Notch functions to maintain progenitor cells in a pluripotent state affecting differentiation, proliferation, and survival. In cancer, Notch gene amplification, chromosomal translocation, or mutation leads to elevated Notch signaling, imparting a growth advantage by keeping tumor cells and tumor stem cells in a pluripotent proliferative state (6). A similar concept is emerging during tumor angiogenesis where Notch signaling directs endothelial cell fate during new vessel formation via the Notch ligands Dll4 and Jag1 (7, 8).

Intramembrane processing is an emerging theme for membrane receptor signaling. γ-Secretase is a key enzyme in the intramembrane proteolytic processing of receptors including the amyloid precursor protein (APP), CD44, HER4, and Notch (9–11). Notch signaling requires plasma membrane receptor interaction (Notch1-4) with one of five transmembrane ligands (Jagged1, Jagged2, Delta-like1, Delta-like3, and Delta-like4) expressed on neighboring cells. This ligand-receptor interaction initiates a series of intramembrane cleavages, the last of which is mediated by the γ-secretase enzyme complex. The γ-secretase processing of Notch produces the active form called intracellular Notch (ICN). ICN translocates to the nucleus and forms part of a larger transcription complex directly altering the expression of key proliferation- and differentiation-specific genes (3). The strategy of blocking Notch signaling via γ-secretase inhibition holds the potential to target tumor cells, tumor stem cells, and tumor endothelial cells. Inhibition of these three key tumor cell populations could eradicate tumor growth and neovascularization, ultimately leading to tumor regression or terminal differentiation (stasis). Although inhibition of Notch is an attractive tumor-targeting strategy, Notch plays an essential physiologic role in regenerative tissues of the hematopoietic system, gastrointestinal tract, and skin (12). Prolonged inhibition of Notch signaling in these target organs can therefore be associated with *in vivo* toxicity.

The present study describes a novel γ-secretase small-molecule inhibitor. RO4929097 is a potent and selective γ-secretase inhibitor targeting cellular Notch processing. RO4929097 is orally active in 7 of 8 established preclinical tumor models, well below the maximum tolerated exposure established in toxicity studies. Importantly, acute intermittent dosing produces sustained efficacy, helping to mitigate toxicity. These preclinical results support the continued development of RO4929097, which is currently undergoing phase I dose escalation in patients with solid tumors.

Note: Supplementary data for this article are available at Cancer Research Online (http://cancerres.aacrjournals.org/).

Requests for reprints: John F. Boylan, Discovery Oncology, Hoffmann-La Roche, Inc., 340 Kingsland Street, Nutley, NJ 07110. Phone: 973-235-3076; Fax: 973-235-6185; E-mail: john.boylan@roche.com.

doi:10.1158/0008-5472.CAN-09-1843

Materials and Methods

Compound. The test compound RO4929097 [2,2-dimethyl-*N*-((*S*)-6-oxo-6,7-dihydro-5H-dibenzo[*b*, *d*]azepin-7-yl)-*N*′-(2,2,3,3,3-pentafluoro-propyl)-malonamide] was synthesized according to the procedure described in patent application (WO2005/023772).

Cell lines. The human cancer cell lines A549, MDA-MB-468, LOVO, BxPC3, HCT-116, AsPC-1, MiaPaCa-2, and Calu-6 were purchased from the American Type Culture Collection. The H460a cell line was a gift from Dr. Jack Roth (M. D. Anderson Medical Center).

***In vitro* potency assays.** The cell-free assay for γ-secretase was done as described (13). The cellular Aβ-lowering assay used human HEK293 cells stably transfected with a vector expressing a cDNA of the human APP wild-type gene (APP695) as described (14). The cellular Notch reporter assay used a stably transfected HEK293 cell line expressing the human Notch1 and luciferase reporter (15). Western blot analysis, soft-agar growth, RNA isolation, and reverse transcription-PCR (RT-PCR) were done using standard laboratory techniques. The catalogue numbers for each probe set were *Hes1* (Hs00172878_m1), *c-myc* (Hs00153408_m1), *p21* (Hs00355782_m1), *ACTB* (4333762F), and *18S* (4319413E). The catalogue information for the Western blot antibodies were ICN (Cell Signaling; 2421) at a dilution of 1:1,000, Hes1 (U.S. Biological; H2034-35) at a dilution of 1:1,000, and actin (Sigma; 5316) at a dilution of 1:10,000.

Xenograft tumor models. The *in vivo* efficacy experiments were conducted as described (16). RO4929097 was formulated as a suspension in 1.0% Klucel in water with 0.2% Tween 80 for oral administration. RO4929097-treated mice were orally dosed with suspensions at 3 to 60 mg/kg RO4929097 according to the indicated regimens. In the Calu-6 xenograft model, RO4929097 was dosed at 60 mg/kg/d every other week for 4 weeks (7+/7- × 2 cycles). For all other xenograft models, RO4929097 was dosed once daily at 10 mg/kg for 21 days. Statistical analysis was determined by Mann-Whitney rank-sum test, one-way ANOVA, and post hoc Bonferroni *t* test (SigmaStat version 2.0; Jandel Scientific). Differences between groups were considered significant when $P \leq 0.05$. A549 tumors from vehicle-treated and selected RO4929097-treated groups were collected and fixed in 10% zinc-formalin overnight, processed, paraffin-embedded, sectioned at 5 μm, and stained with H&E for histopathology assessment. An Olympus BX51 microscope (×40 objective) mounted with a Nikon DS-Fi1 using the NIS-Elements F2.20 program collected the histology pictures. For Western blot analysis, three A549 tumors from each group, 7 (60 mg/kg) or 21 days (3 and 30 mg/kg), were flash-frozen. Collagen type V was detected using the H-200 antibody from Santa Cruz Biotechnology at a dilution of 1:1,000, and MFAP5 was detected using the antibody from Abnova at a dilution of 1:1,000.

Angiogenesis RT-PCR array. cDNA samples prepared for Affymetrix analysis were analyzed with the 384-well mouse angiogenesis PCR array in duplicate (SABioscienses) according to the manufacturer's protocol.

Microarray method. A549 and H460a cells were treated with either RO4929097 or vehicle and harvested at 6 and 24 h. Total RNA was isolated using the Qiagen RNeasy Mini Kit (Qiagen) and quality was assessed on the Agilent Bioanalyzer 2100. Total RNA (15 μg) was converted into cDNA and cRNA according to the manufacturer's protocol. For the statistical analysis of the expression measurements, an in-house implementation of the RMA algorithm (17) was used to perform the background correction, normalization, and signal summarization. Differentially expressed genes were further analyzed using the Gene Set Enrichment Analysis algorithm (18) implemented by the NextBio software (NextBio).

Results

RO4929097 has potent γ-secretase *in vitro* inhibitory activity. RO4929097 is a potent and selective inhibitor of the γ-secretase enzyme complex. The primary dibenzazepinone core was derived from LY411575 (19). Medicinal chemistry efforts produced RO4929097 showing strong potency, selectivity, and drug-like properties. Multiple *in vitro* assays were used to characterize the potency and selectivity of RO4929097 (Fig. 1*A*). The primary *in vitro* assay used human cell-free membrane preparations to provide the γ-secretase enzyme complex. RO4929097 strongly inhibited γ-secretase enzyme activity with a 4 nmol/L potency (IC_{50}; Fig. 1*B*). The cellular processing of APP was measured using an ELISA readout. HEK293 cells were engineered to overexpress APP. Processing was measured by an ELISA-based quantitation of the Aβ 1-40 γ-secretase product. Treatment of cells caused a dose-dependent decrease in the amount of Aβ peptides secreted into the culture medium. Figure 1*B* shows a representative data set (EC_{50}, 14 ± 4 nmol/L; $n = 4$). Cellular Notch inhibitory activity was measured using a HEK293 cell line stably expressing a truncated human Notch1 fused in the intracellular domain to a VP16/Gal14 transcriptional activator, which drives a firefly luciferase gene. Inhibition of Notch processing produced a reduction in luciferase reporter activity as measured by chemiluminescence. The potent *in vitro* activity of RO4929097 translated into strong dose-dependent inhibition of Notch processing in the Notch cell-based reporter assay (EC_{50}, 5 ± 1 nmol/L; $n = 5$). The potency of RO4929097 in cell-free and cellular assays was in the low nanomolar range with >100-fold selectivity observed with respect to 75 other proteins of various types including receptors, ion channels, and enzymes (CEREP panel; data not shown). No *in vitro* inhibitory activity was observed on the closely related cathepsin D and BACE aspartyl proteases (data not shown).

RO4929097 inhibits Notch processing in human tumor-derived cells. Formation of the ICN protein following Notch receptor cleavage by γ-secretase is a critical step in Notch signaling (3–5). ICN moves to the nucleus becoming part of a larger transcriptional complex regulating the expression of various target genes including *Hes1*. A549 non–small cell lung carcinoma (NSCLC)–derived cells were treated with RO4929097 for 24 h. The reduction in *Hes1* mRNA levels was detected as early as 2 h following compound treatment and showed a dose-dependent reduction beginning at 100 nmol/L (Fig. 2*A*). The reduction in expression of ICN protein and the Notch target gene product, *Hes1*, was monitored by Western blot. After 5 days of treatment, RO4929097 suppressed the production of ICN in the human NSCLC A549 cells inducing a flattened and less transformed tumor cell phenotype in tissue culture (Fig. 2*B* and *C*). The morphology was reminiscent of nontransformed primary bronchial epithelia cells grown in tissue culture. A variety of tumor cell lines were treated with RO4929097 including colon, breast, melanoma, and pancreatic cell lines. All of the cell lines exhibited a similar flattened, less transformed phenotype (data not shown). This translated into a dose-dependent reduction in soft-agar growth in the MDA-MB-468 cell line (Fig. 2*D*). Interestingly, the appearance of an apoptotic phenotype following compound treatment was not observed. Cells grown in the presence of RO4929097 showed little effect on overall growth (data not shown). Fluorescence-activated cell sorting analysis documents a modest cell cycle slowing at 5 μmol/L for 72 and 120 h (Supplementary Fig. S1; Supplementary Table S1). RO4929097 did not completely block tumor cell proliferation nor induce apoptosis but instead elicited a slower-growing phenotype. This mechanism is consistent with cellular Notch inhibition and analogous to the role of Notch during normal tissue development where progenitor cells adopt a new phenotype while continuing to proliferate (5).

***In vivo* efficacy of RO4929097.** The preclinical antitumor activity was tested in the A549 NSCLC xenograft model using a variety of doses and schedules in an attempt to ameliorate the anticipated toxicities associated with inhibition of Notch signaling

in normal tissues such as in the gastrointestinal tract. Oral administration of 3 to 60 mg/kg RO4929097 once daily (Fig 3*A*) or twice daily (data not shown) to nude mice bearing A549 NSCLC xenografts for either 7, 14, or 21 days of a 21-day schedule resulted in significant tumor growth inhibition compared with vehicle-treated animals (Fig. 3*A*). The tumor growth inhibition values ranged from 66% to 91% ($P < 0.001$). Importantly, the antitumor effects were sustained after dosing was completed.

When mice were treated with 60 mg/kg RO4929097 twice daily with the 7+/14- schedule, treatment initially caused regression of established A549 tumors. At the end of the 21-day cycle (day 47), tumor growth inhibition was still 91% compared with vehicle control mice. Inhibition of tumor growth remained prolonged and sustained up to 34 days post-treatment (day 67). On day 67, these mice were retreated with the same dose of RO4929097 for a second cycle (7 days) until day 74 (Fig. 3*B*). Tumor growth continued to be inhibited out to day 90. Similar results were observed when RO4929097 was administered once daily or twice daily consecutively for 21 days, with treatment ending on day 47 post-tumor implant. For all 21-day treated groups, inhibition of tumor growth remained prolonged and sustained. It is of note that whether RO4929097 was dosed once daily (Fig. 3*C*) or twice daily (data not shown) with either the 14+/7- or full 21-day treatment schedule, there was a general lack of dose response observed with respect to tumor growth inhibition (Fig. 3*C*). Exposures producing efficacy ($AUC_{24\ h}$) were ~1,100 ng h/mL after an oral daily dosing schedule of 10 mg/kg/d for 21 days. No change in exposure was observed between days 1 and 21 (data not shown). The pharmacokinetics of RO4929097 in mouse was characterized by a moderate to high plasma clearance, high volume of distribution, and moderate to high oral bioavailability.

The observed antitumor efficacy was unique compared with that observed with other cancer therapeutics in that the efficacy was prolonged after cessation of treatment and the maximal efficacy was sometimes observed 1 or 2 weeks after treatment ceased. This *in vivo* response supports a rationale around cyclical dosing in the clinic. Both continuous daily and intermittent schedules were efficacious without toxic (>20%) body weight loss (Supplementary Fig. S2). However, there was less body weight loss in mice on the intermittent schedule possibly due to the recovery of normal stem cells.

Selected A549 tumors were collected at the end of the study for histology assessment, Western blot analysis, and angiogenesis gene analysis to further investigate the mechanism of action. Histologic analysis of tumors harvested at the end of this study revealed large areas of necrosis with an increase in extracellular matrix (Fig. 4*A*).

Microarray analysis revealed mRNA expression changes consistent with extracellular matrix alteration (data not shown). RO4929097-treated tumors were harvested for Western blot analysis (Fig. 4*B*). Collagen type V expression was significantly reduced, whereas MFAP5 protein expression was elevated. Collagen type V and MFAP5 are structural proteins that make up the extracellular matrix. The expression of the ICN was reduced consistent with inhibiting Notch processing *in vivo*. Interestingly, total Notch1 protein levels were also reduced, suggesting a possible feedback loop where Notch regulates its own expression. The inhibition of Notch ICN cleavage was somewhat reduced at the high dose of 60 mg/kg. The loss of ICN inhibition is not unexpected because these samples were collected at the end of the 21-day study. This group of animals was on a 7-day dosing schedule and had not been dosed for 14 days. This in contrast to the 3 and 30 mg/kg groups, which were on a 14-day dosing schedule and had not been dosed for 7 days before tumor harvest.

Notch signaling has been reported to play a role in tumor angiogenesis. RO4929097 produced a dose-dependent inhibition of tubule formation in the cell-based AngioKit assay (data not shown). An angiogenesis-specific RT-PCR array was used to investigate the

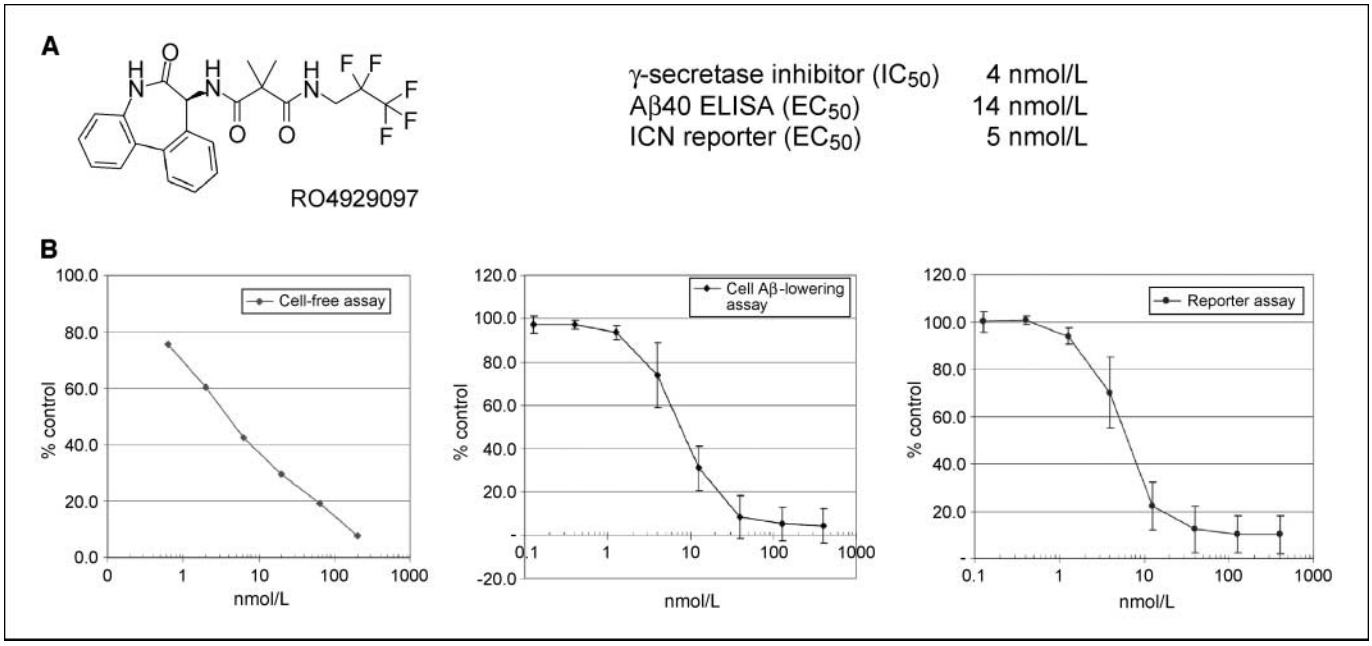

Figure 1. RO4929097 chemical structure and *in vitro* Aβ40 and Notch potency. *A,* RO4929097 was derived from a dibenzazepinone lead. *B,* RO4929097 was assayed in a cell-free γ-secretase enzyme assay and two cellular assays using engineered cell lines to monitor Aβ40 and Notch processing.

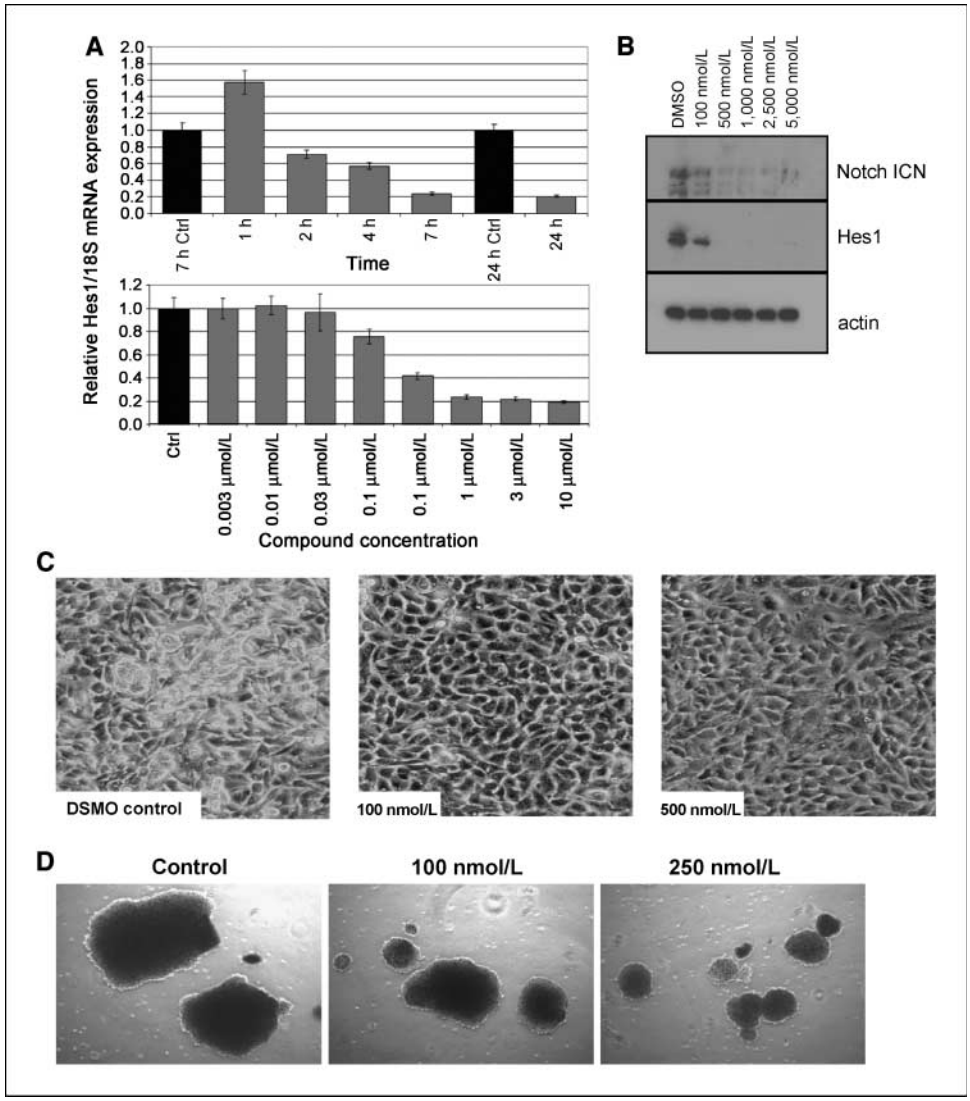

Figure 2. RO4929097 inhibits the production of ICN, reducing the expression of the downstream Notch target *Hes1*, producing a less transformed morphology in A549 cells. *A,* RT-PCR analysis was used to monitor *Hes1* mRNA expression. *B,* Western blot analysis was used to monitor the protein expression of ICN and Hes1. *C,* tissue culture pictures showing a less transformed morphology. *D,* RO4929097 reduces the size of MDA-MB-468 soft agar colonies. Pictures were taken 3 weeks after start of dosing. Compound was added twice weekly.

effect of RO4929097 on xenograft angiogenesis gene expression. An important control was the inclusion of the H460a xenograft because this model is nonresponsive to the *in vivo* inhibitory effects of RO4929097 (Fig. 3*D*). Figure 4C presents the array data showing a reduction in several key angiogenic mRNAs following compound treatment *in vivo* including *VEGFR2* (*KDR*), *CD31* (*PECAM1*), and *JAG1*. Interestingly, there was little change in the angiogenic genes survey for the H460a xenograft as expected given the lack of efficacy in this model. These data are consistent with an antiangiogenic mechanism of action for RO4929097.

Additional preclinical antitumor activity was evaluated in several xenograft models using a standard daily dose of 10 mg/kg to allow cross-study comparison of efficacy (Fig. 3*D*). RO4929097 is orally active in 6 of 7 established tumor models in nude mice dosed below the maximum tolerated dose on a daily schedule for 21 days and is orally active in a seventh model on an intermittent schedule (Calu-6 model dosed at 60 mg/kg 7+/7- × 2 cycles). The lack of efficacy in the H460a cell line serves as the basis for identifying a responder/nonresponder molecular signature for RO4929097.

Pharmacodynamic effect of γ-secretase inhibition using a rat hair follicle assay. Notch signaling occurs in a variety of normal tissues as part of the cell differentiation and regeneration process. Our mRNA expression analysis revealed the hair follicle as a tissue that uses the Notch signaling axis (data not shown), consistent with published reports (20, 21). The hair follicle may represent a surrogate tissue that could be used to monitor Notch inhibition during clinical development of RO4929097. We sought to first validate this approach by developing a RT-PCR assay to monitor the Notch target gene, *Hes1*, in hair follicles following RO4929097 *ex vivo* dosing. Both donor hair follicle mRNAs showed a significant decrease in *Hes1* mRNA expression and no change in *c-myc* mRNA expression following compound treatment (Fig. 5*A* and *B*).

Key *in vivo* validation of this approach was achieved using a rat hair follicle regrowth assay. A section of hair on the back of a Fischer rat was removed because rodent hair follicles normally exist in the resting telogen phase. Hair removal stimulates regrowth and the hair follicles enter a period of growth and differentiation called the anagen phase (20). Rats were dosed orally at 6 mg/kg on a daily schedule and hair was harvested at the indicated times (Fig. 5*C, black triangles*). Plasma exposures ranged from 111 to 176 ng/mL 2 h post-dose during the course of the experiment in line with previous data. *Hes1* mRNA levels were decreased by

24 h and remained reduced through the course of the experiment (Fig. 5*D*). The *c-myc* and *p21* mRNAs showed no expression change in response to dosing.

Comparative microarray analysis of RO4929097 transcriptional effect. Inhibition of Notch signaling holds the potential to inhibit three key areas of tumor survival: tumor cell growth, tumor stem cell repopulation, and tumor angiogenesis (6, 7). It remains unclear which of these pathways or a combination of inhibiting these pathways drives efficacy following Notch inhibition. To begin to address this question, comparative microarray analysis of RO4929097-treated A549 (sensitive) and H460a (resistant) cells was initiated. This analysis used two short-term time points of 6 and 24 h post-treatment. It was reasoned that direct effects of RO4929097 would occur within 24 h of treatment after which secondary mRNA changes would complicate the analyses. A549 cells treated for 6 h showed changes in gene expression, which fell into three main categories: transcription factors and repressors, heat shock protein binding, and vasculature development (Fig. 6*A*). Treatment for 24 h expanded these categories to include genes related to extracellular matrix, cell differentiation, metastasis, and cell-cell signaling. Specific genes listed in the boxes represent mRNAs that were altered at both 6 and 24 h. Some of the specific mRNA changes include three well-known Notch-regulated transcription factors *Hes1, Hes4*, and *Hey1*, the expression of which was reduced after RO4929097 treatment. Several genes were induced following RO4929097 treatment including *Agr2, Arid5B, Megf9, Ell2, Gch1*, and *IL6R*. Interestingly, the *in vivo* nonresponsive H460a cell line did not show *Hes1, Hes4*, or *Hey1* significant mRNA reduction and had a very quiet gene expression pattern. A Gene Set Enrichment Analysis was done using the NextBio software to identify gene sets having a significant correlation between RO4929097-induced gene changes and primary tumors. Our analysis used the large data set derived from a multisite clinical study involving hundreds of NSCLC patients and highlighted several groups of genes associated with different stages of NSCLC (22). For example, an overall positive correlation (*P*-value = 1.7E-9) was observed between the RO4929097-induced gene signature at 24 h and that derived from a comparison between well-differentiated and poorly differentiated non–small cell lung adenocarcinomas (Fig. 6*B*). Overall, the microarray analyses detected the expression of genes associated with a less transformed phenotype following RO4929097 treatment.

Discussion

Growing preclinical evidence shows that inactivation of the Notch pathway by targeting γ-secretase may be a viable strategy for

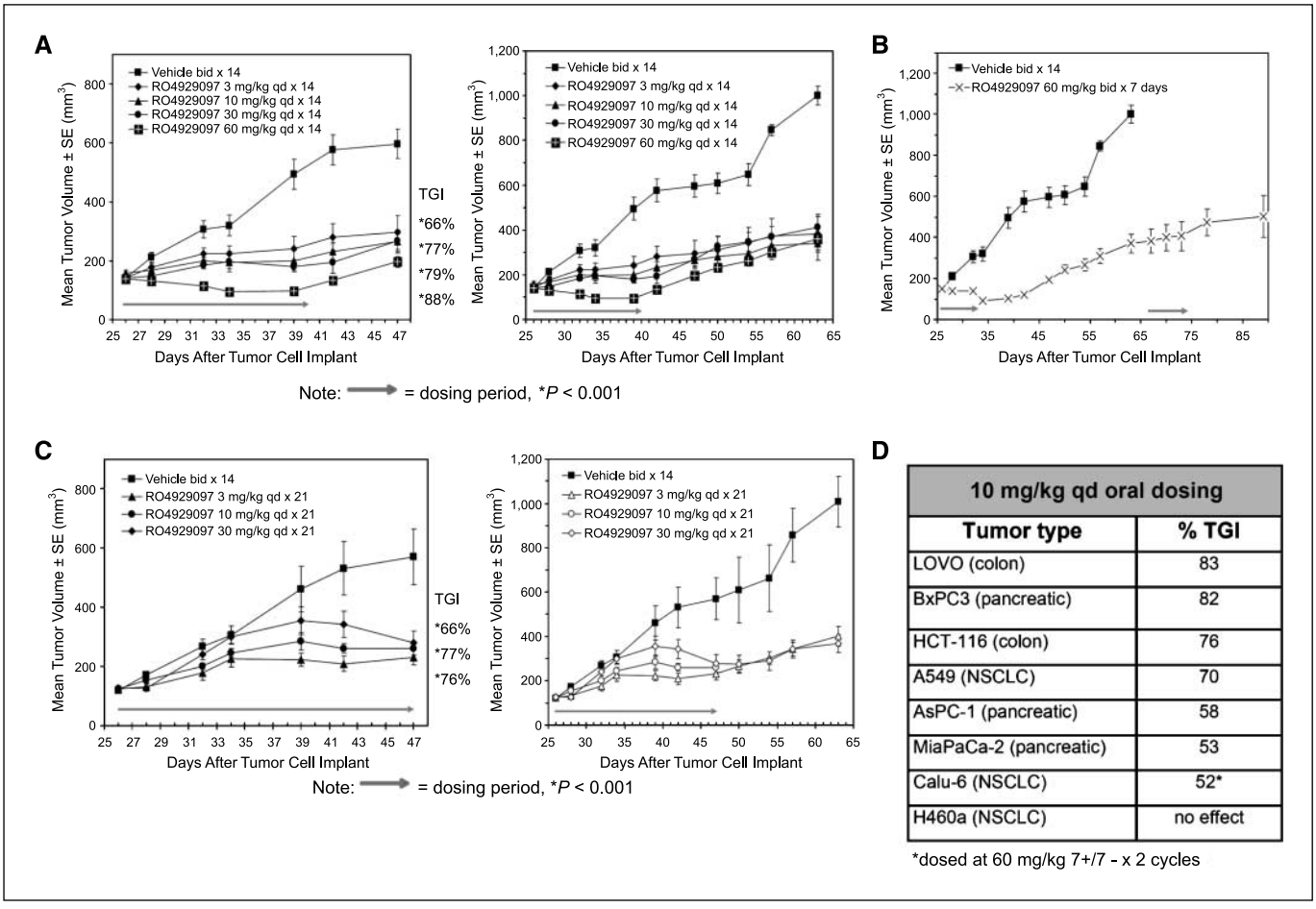

Figure 3. *In vivo* efficacy of RO4929097 in the A549 xenograft model. *A,* nude mice bearing A549 s.c. tumors were dosed orally following the indicated schedule. *Arrow,* length of treatment. *B,* animals from the 60 mg/kg group were monitored after cessation of treatment for 32 d and then redosed for 7 d. *C,* animals were dosed on a daily 21-day schedule at the indicated concentrations and then monitored after cessation of treatment. *D,* summary of breadth of *in vivo* efficacy. *TGI,* tumor growth inhibition; *bid,* twice daily; *qd,* once daily.

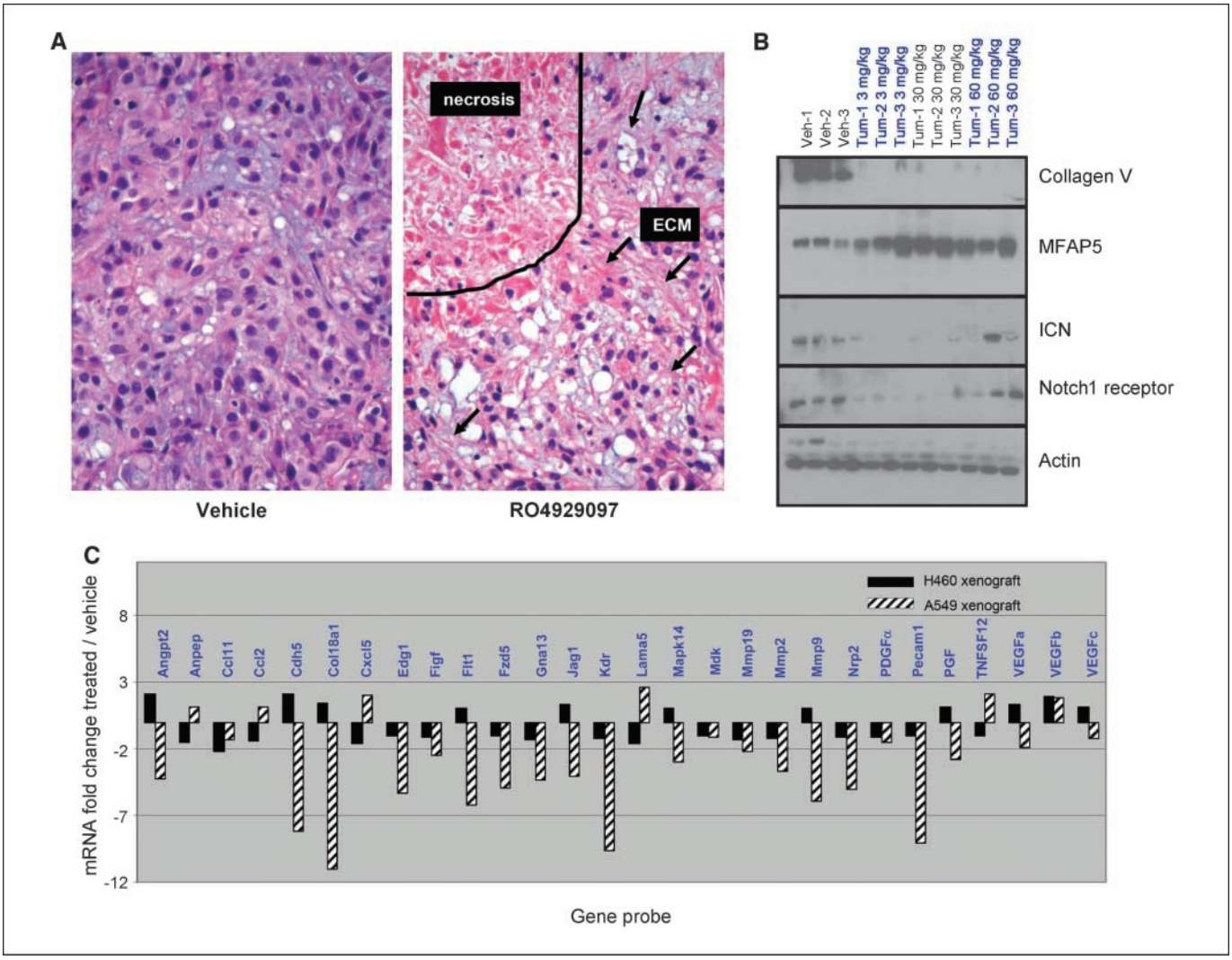

Figure 4. RO4929097-treated A549 tumors have increased areas of necrosis with relative increase in extracellular matrix (*ECM*). *A,* representative H&E-stained tumor tissue sections from vehicle and 10 mg/kg/d × 21 d RO4929097-treated groups. *B,* Western blot analysis of xenograft protein was done. *C,* angiogenesis-specific RT-PCR array showing down-regulation of several angiogenic genes in the sensitive A549 xenograft model compared with the insensitive H460a model.

the treatment of cancer (6). RO4929097 was originally developed for Alzheimer's disease as a potent inhibitor of γ-secretase targeting APP processing. This article reports the cross-therapeutic application of RO4929097 to cancer treatment via inhibition of γ-secretase-mediated processing of Notch signaling.

RO4929097 is a potent and selective γ-secretase small-molecule inhibitor targeting the Notch signaling pathway resulting in decreased ICN production and mRNA expression of the ICN target gene, *Hes1*, in tumor cells. Addition of RO4929097 to tumor-derived cell lines produced a flattened, less transformed phenotype as well as a reduced capability for soft-agar growth. This is in good agreement with data from Stylianou and colleagues, which reported a less transformed phenotype and loss of ability to grow in soft agar when Notch signaling was inhibited by the over-expression of the Notch negative regulator Numb in breast cancer cells (23). RO4929097 produced efficacy when dosed orally in 7 of 8 xenograft models. This efficacy was sustained in the absence of further dosing and was not associated with body weight loss in mice. The data provided experimental support for proceeding into clinical development using intermittent dosing, which may allow for recovery in normal tissue from Notch inhibition while maintaining tumor efficacy. This hypothesis will be tested during clinical development using a hair follicle pharmacodynamic assay to monitor Notch inhibition.

An important aspect of oncology clinical development is the understanding of what factors contribute to efficacy. The role of Notch in cell fate determination points to three potential drivers of efficacy in tumors: (*a*) promoting tumor cell differentiation, (*b*) reducing the cancer stem cell tumor subpopulation, and (*c*) inhibiting angiogenesis by targeting Notch signaling in tumor endothelial cells (3–8). A better understanding of this biology will undoubtedly affect the clinical development of γ-secretase inhibitors.

The effect of Notch signaling in tumor cells is a growing area of investigation. Notch signaling has been shown to play a role in the maintenance of tumor stem cells as well as playing a role in maintaining tumor cells in a less differentiated, highly proliferative state (1, 6). As an approach to study the mechanism of action of RO4929097, gene analysis experiments were done on the sensitive (A549) and resistant (H460a) tumor cell lines. After 6 h of

compound treatment, down-regulation of several transcription factor mRNAs was observed including *Hes1, Hes4*, and *Hey1* in the A549 responder cell line in contrast to the H460a nonresponder. After 24 h of treatment, the list of affected genes expanded to include mRNAs related to extracellular matrix, cell differentiation, metastasis, and cell-cell signaling. This is consistent with the xenograft experiment where collagen type V protein expression was reduced, whereas MFAP5 protein expression was elevated. Both of these proteins are components of the extracellular matrix. Collagen type V expression is often reduced and MFAP5 expression is often elevated in normal tissues (24–28). MFAP5 is a key component of microfibrils, which provide elasticity in such tissues as lung and skin. In addition to the role in elastic fibers, MFAP5 participates in Notch signaling through a direct interaction with the Notch receptor (29). Recent data suggest that MFAP5 antagonizes Notch signaling, promoting endothelial cell sprouting (30).

Comparing the entire RO4929097-induced gene signature to the existing public expression data sets in NextBio showed that many gene changes observed in tumor cell differentiation were also changed in RO4929097-treated cells. These data are consistent with the working hypothesis that Notch1 inhibition in A549 tumor cells leads to a differentiated phenotype (Fig. 6*B*). It is difficult to assess the effect of RO4929097 on cancer stem cells in this cell model system. It is interesting to note that RO4929097 treatment induced the expression of the interleukin-6 receptor (Fig. 6*A*). Interleukin-6 supports cancer stem cell renewal in breast cancer mammospheres via Notch3 (31). The increase in the interleukin-6 receptor following RO4929097 may represent a regulatory compensation for the loss of Notch signaling.

Notch signaling and tumor vascularization are the most compelling aspects of Notch tumor biology to date. Tumor endothelial cells use Notch signaling in building the tumor vasculature analogous to the role of Notch in cell fate determination during development (7, 8). The current understanding of Notch signaling during tumor angiogenesis suggests that the Notch axis plays a determining role in helping tumor endothelial cells adopt either a tip or tube phenotype at critical points during angiogenesis. This cell-cell communication and cell signaling are carried out in conjunction with vascular endothelial growth factor signaling to generate and then finely tune the mature vessels. The molecular analysis of xenografts treated with RO4929097 show reduced expression of genes associated with angiogenesis, consistent with the ability of RO4929097 to inhibit tumor angiogenesis including *VE-cadherin* (*Cdh5*), *VEGFR1* (*FLT1*),

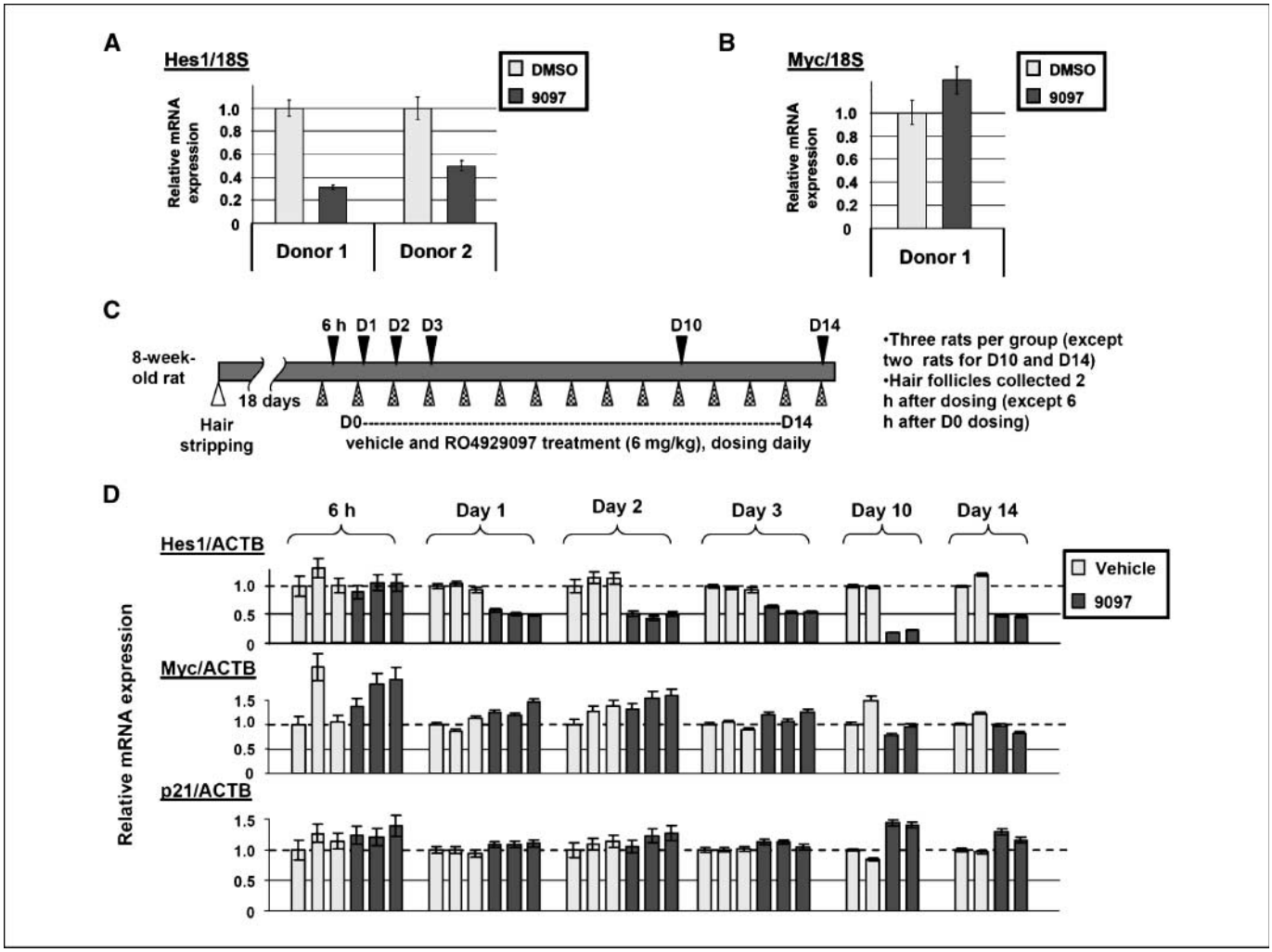

Figure 5. *Hes1* mRNA can serve as a pharmacodynamic marker for tracking Notch inhibition in hair follicles. *A, Hes1* mRNA expression change in *in vitro* treated human hair follicles (2 μmol/L). *B, c-myc* mRNA expression. *C,* schematic representation of *in vivo* treatment of rats. *D,* rat *Hes1, c-myc*, and *p21 in vivo* mRNA expression changes.

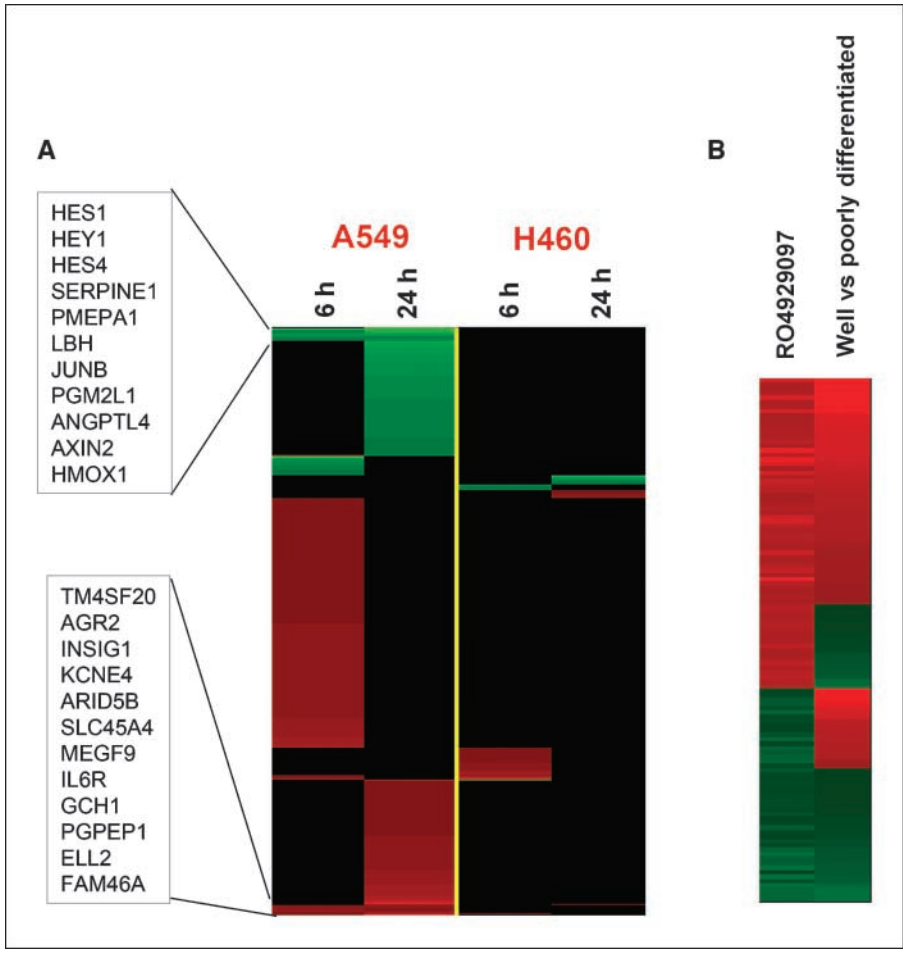

Figure 6. Comparative microarray analysis. *A,* heat map of human gene expression changes induced by RO4929097 at 6 and 24 h in A549 and H460 NSCLC-derived cell lines as monitored (Affymetrix U133 Plus 2 arrays). *Red* and *green,* genes up-regulated and down-regulated at least 1.5-fold after RO4929097 treatment ($P < 0.001$, ANOVA, compared with untreated controls), respectively. Boxes list mRNAs that were altered at both 6 and 24 h. *B,* heat map of genes that are differentially expressed in both RO4929097-treated A549 cells (versus untreated) and well-differentiated non–small cell lung adenocarcinomas (versus poorly differentiated) identified by Gene Set Enrichment Analysis using the NextBio software.

VEGFR2 (*KDR*), *MMP9*, and *CD31* (*PECAM1*; Fig. 4*C*). Large pockets of necrosis are present in xenograft tumors, also consistent with an antiangiogenic mechanism. These results are similar to those reported for the Notch1 decoy (32). The *in vivo CD31* and *VE-cadherin* expression was reduced and tumor growth was inhibited in the absence of Notch1 function.

It is important to note that γ-secretase is a promiscuous protease enzyme complex with up to 60 potential substrates in addition to Notch (33, 34). RO4929097 and other reported γ-secretase inhibitors likely carry additional inhibitory activities that preclude a complete understanding of Notch tumor biology at this time. Differences in substrate selectivity can explain some differences in biology reported for other γ-secretase inhibitors such as cell cycle inhibition (35). Cell context is likely a key determinate of how a cell responds to Notch inhibition. Interestingly, selective small-molecule inhibitors targeting APP processing over Notch processing have been reported and remain an area of great interest in Alzheimer's disease (36, 37). It remains to be determined whether RO4929097 inhibits all four Notch family members and what other substrates might be preferentially inhibited by RO4929097. A deeper understanding of Notch receptor selectivity will likely affect clinical development of γ-secretase inhibitors given the potential for different biology within the Notch receptor family (38).

RO4929097 is currently being tested in a phase I multidose escalation in patients with solid tumors using several pharmacodynamic readouts including the *Hes1* hair follicle assay. As an oral agent, two schedules are being evaluated to exploit the inherent flexibility of oral dosing and minimize toxicity (39). Preclinical data suggest that antitumor effects may continue to develop over time and efficacy may be sustained in the absence of further dosing. How this can be best exploited in the clinic remains to be determined especially given the function of Notch signaling in normal tissues. Targeted inhibition of Notch signaling has the potential to affect tumor angiogenesis, tumor cell differentiation, and survival of tumor stem cells. The H460a cell line appears to be refractory to the effects of RO4929097. A better understanding of the molecular defects driving the resistance of the H460a cell line may provide a deeper understanding of the Notch signaling pathway in cancer. This will lay the research groundwork for a patient selection molecular profile. Further evaluation of the key drivers of efficacy will provide important information on the types of tumors responsive to treatment and appropriate selection of patients who are most likely to derive clinical benefit from RO4929097.

Disclosure of Potential Conflicts of Interest

No potential conflicts of interest were disclosed.

Acknowledgments

Received 5/19/09; revised 8/5/09; accepted 8/5/09; published OnlineFirst 9/22/09.

The costs of publication of this article were defrayed in part by the payment of page charges. This article must therefore be hereby marked *advertisement* in accordance with 18 U.S.C. Section 1734 solely to indicate this fact.

We thank Huifeng Niu for discussions and critical evaluation of the article.

References

1. Telerman A, Amson R. The molecular programme of tumor reversion: the steps beyond malignant transformation. Nat Cancer Rev 2009;9:206–15.
2. Sell S. Stem cell origin of cancer and differentiation therapy. Crit Rev Oncol Hematol 2004;51:1–28.
3. Tien A, Rajan A, Bellen HJ. A Notch updated. J Cell Biol 2009;184:621–9.
4. Borggrefe T, Oswald F. The notch signaling pathway: transcriptional regulation at Notch target genes. Cell Mol Life Sci 2009;66:1631–46.
5. D'Souza B, Miyamoto A, Weinmaster G. The many facets of notch ligands. Oncogene 2008;27:5148–67.
6. Rizzo P, Osipo C, Forman K, et al. Rationale targeting of notch signaling in cancer. Oncogene 2008;27:5124–31.
7. Phng L-K, Gerhardt H. Angiogenesis: a team effort coordinated by Notch. Dev Cell 2009;16:196–208.
8. Dufraine J, Funahashi Y, Kitajewski J. Notch signaling regulates tumor angiogenesis by diverse mechanisms. Oncogene 2008;27:5132–7.
9. Kopan R, Ilagan MX. γ-secretase: proteasome of the membrane? Nat Rev Mol Cell Biol 2004;5:499–504.
10. Steiner H, Fluhrer R, Haass C. Intramembrane proteolysis by γ-secretase. J Biol Chem 2008;283: 29627–31.
11. Tolia A, DeStrooper B. Structure and function of γ-secretase. Semin Cell Dev Biol 2009;20:211–8.
12. Purow B. Notch inhibitors as a new tool in the war on cancer: a pathway to watch. Curr Pharm Biotechnol 2009;10:154–60.
13. Li Y-M, Lai M-T, Xu M, et al. Presenilin 1 is linked with γ-secretase activity in the detergent solubilized state. Proc Natl Acad Sci U S A 2000;97:6138–43.
14. Wolfe MS, Kopan R. Intramembrane proteolysis: theme and variations. Science 2004;305:1119–23.
15. Brockhaus M, Grunberg J, Rohrig S, et al. Neuro-Report 1998;9:1481–6.
16. Higgins B, Kolinsky K, Linn M, et al. Antitumor activity of capecitabine and bevacizumab combination in a human estrogen receptor-negative breast adenocarcinoma xenograft model. Anticancer Res 2007;27:2279–88.
17. Irizarry RA, Bolstad BM, Collin F, et al. Summaries of Affymetrix GeneChip probe level data. Nucleic Acids Res 2003;31:1–8.
18. Subramanian A, Tamayo P, Mootha VK, et al. Gene set enrichment analysis: a knowledge-based approach for interpreting genome-wide expression profiles. Proc Natl Acad Sci U S A 2005;102:15545–50.
19. Peters J-U, Galley G, Jacobsen H, et al. Novel orally active, dibenzazepinone-based γ-secretase inhibitors. Bioorg Med Chem Lett 2007;17:5918–23.
20. Schneider MR, Ullrich RS, Paus R. The hair follicle as a dynamic miniorgan. Curr Biol 2009;19:R132–42.
21. Demehri S, Kopan R. Notch signaling in bulge stem cells is not required for selection of hair follicle fate. Development 2009;136:891–6.
22. Shedden K, Taylor JM, Enkemann SA, et al.; Director's Challenge Consortium for the Molecular Classification of Lung Adenocarcinoma. Gene expression-based survival prediction in lung adenocarcinoma: a multi-site, blinded validation study. Nat Med 2008;14:822–7.
23. Stylianou S, Clarke RB, Brennan K. Aberrant activation of Notch signaling in human breast cancer. Cancer Res 2006;66:1517–25.
24. Penner AS, Rock MJ, Kielty CM, Shipley JM. Microfibril-associated glycoprotein-2 interacts with fibrillin-1 and fibrillin-2 suggesting a role for MAGP-2 in elastic fiber assembly. J Biol Chem 2002;277: 35044–9.
25. Wenstrup RJ, Florer JB, Brunskill EW, et al. Type V collagen controls the initiation of collagen fibril assembly. J Biol Chem 2004;279:53331–7.
26. Marian B, Danner MW. Skin tumor promotion is associated with increased type V collagen content in the dermis. Carcinogenesis 1987;8:151–4.
27. Barsky SH, Rao CN, Grotendorst GR, Liotta LA. Increased content of type V collagen in demoplasia of human breast carcinoma. Am J Pathol 1982;108: 276–83.
28. Fischer H, Stenling R, Rubio C, Lindblom A. Colorectal carcinogenesis is associated with stromal expression of COL1A1 and COL5A2. Carcinogenesis 2001;22:875–8.
29. Miyamoto A, Lau R, Hein PW, Shipley JM, Weinmaster G. Microfibrillar protein MAGP-1 and MAGP-2 induce Notch1 extracellular domain dissociation and receptor activation. J Biol Chem 2006;281:10089–97.
30. Albig AR, Becenti DJ, Roy TG, Schiemann WP. Microfibril-associate glycoprotein-2 (MAGP-2) promotes angiogenic cell sprouting by blocking notch signaling in endothelial cells. Microvasc Res 2008;76:7–14.
31. Sansone P, Storci G, Tavolari S, et al. IL-6 triggers malignant features in mammospheres from human ductal breast carcinoma and normal mammary gland. J Clin Invest 2007;117:3988–4002.
32. Funahashi Y, Hernandez SL, Das I, et al. A Notch1 ectodomain construct inhibits endothelial Notch signaling, tumor growth, and angiogenesis. Cancer Res 2008;68:4727–35.
33. Gordon WR, Arnett KL, Blacklow SC. The molecular logic of Notch signaling—a structural and biochemical perspective. J Cell Sci 2008;121:3109–19.
34. Beel AJ, Sanders CR. Substrate specificity of γ-secretase and other intramembrane proteases. Cell Mol Life Sci 2008;65:1311–34.
35. Rao SS, O'Neil J, Liberator CD, et al. Inhibition of Notch signaling by γ secretase inhibitor engages the RB pathway and elicits cell cycle exit in T-cell acute lymphoblastic leukemia cells. Cancer Res 2009;69: 3060–8.
36. Mayer SC, Kreft AF, Harrison B, et al. Discovery of Begacestat, a Notch-sparing γ-secretase inhibitor for the treatment of Alzheimer's disease. J Med Chem 2008;51: 7348–51.
37. Petit A, Bihe F, Alves da Costa C, et al. New protease inhibitors preventγ-secretase-mediated production of Aβ40/42 without affecting notch cleavage. Nat Cell Biol 2001;3:507–11.
38. Bellavia D, Checquolo S, Campese AF, et al. Notch3: from subtle structural differences to functional diversity. Oncogene 2008;27:5092–8.
39. Martinelli G, Soverini S, Iacobucci I, Baccarani M. Intermittent targeting as a tool to minimize toxicity of tyrosine kinase inhibitor therapy. Nat Clin Pract 2009;6: 68–9.